JACS
JOURNAL OF THE AMERICAN CHEMICAL SOCIETY
Communication
pubs.acs.org/JACS

Synthesis, Characterization, and Reactivity of Hypochloritoiron(III) Porphyrin Complexes

Zhiqi Cong,[†] Sachiko Yanagisawa,[‡] Takuya Kurahashi,[†] Takashi Ogura,[‡] Satoru Nakashima,[‡] and Hiroshi Fujii*[,†]

[†]Institute for Molecular Science and Okazaki Institute for Integrative Bioscience, National Institutes of Natural Sciences, Myodaiji, Okazaki 444-8787, Japan

[‡]Department of Life Science and Picobiology Institute, Graduate School of Life Science, University of Hyogo, Koto, Kamigori, Ako, Hyogo 678-1297, Japan

Supporting Information

ABSTRACT: A hypochloritoiron(III) porphyrin species has been proposed as a key intermediate in an antimicrobial defense system in neutrophils and in heme-catalyzed chlorination reactions. We report herein the preparation, spectroscopic characterization, and reactivity of the bis(hypochlorito)iron(III) porphyrin complex $[(TPFP)Fe^{III}(OCl)_2]^-$ (**1**) and the imidazole−hypochloritoiron complexes $(TPFP)Fe^{III}(OCl)(1\text{-R-Im})$ [R = CH_3 (**2**), H (**3**), CH_2CO_2H (**4**)], in which TPFP is 5,10,15,20-tetrakis(pentafluorophenyl)porphyrinate. The structures of **1**−**4** were confirmed by absorption, ^2H and ^{19}F NMR, EPR, and resonance Raman spectroscopy and electrospray ionization mass spectrometry at low temperature. The reactions of **1** and **2** with various organic substrates show that **1** and **2** are capable of chlorination, sulfoxidation, and epoxidation reactions and that **1** is much more reactive with these substrates than **2**.

Myeloperoxidase (MPO) and chloroperoxidase (CPO) are unique heme peroxidases that catalyze the oxidation of Cl^- to hypochlorite ion (OCl^-).[1−3] MPO is located in the azurophil granules of neutrophils and produces OCl^- or HOCl, which works as an antimicrobial agent, from H_2O_2 and Cl^-.[1,2] On the other hand, CPO is an enzyme of *Caldariomyces fumago* and catalyzes chlorination reactions in the biosynthesis of the chlorinated metabolite caldariomycin.[1,3] It has been proposed that ferric MPO and CPO initially react with H_2O_2 to form an oxoiron(IV) porphyrin π-cation radical species known as compound I.[4] This reacts with Cl^- to form a transient hypochloritoiron(III) porphyrin intermediate, which finally releases HOCl upon protonation of the heme-bound OCl^-.[1−5] In addition, hypochloritometal complexes have been proposed as key intermediates in catalytic oxygenation reactions catalyzed by transition-metal complexes.[6] Because of its significant importance, a hypochloritoiron(III) porphyrin intermediate has been examined for detection in MPO and CPO reactions and in the synthesis of its model complex.[5,7,8] Although previous reports have indicated the possibility of forming hypochloritoiron(III) porphyrin intermediates,[8,9] spectroscopic evidence for such species has not been reported to date. The reactivity of hypochloritoiron(III) porphyrin complexes has also received much attention in relation to those of other terminal oxidant−metal complexes containing OCl^-, hydroperoxide, or iodosylarene as the oxidant.[10] Herein we report the preparation, spectroscopic characterization, and reactivity of the bis(hypochlorito)iron complex $[(TPFP)Fe^{III}(OCl)_2]^-$ (**1**) and the imidazole (Im)−hypochloritoiron complexes $(TPFP)Fe^{III}(OCl)(1\text{-R-Im})$ [R = CH_3 (**2**), H (**3**), CH_2CO_2H (**4**)], in which TPFP is 5,10,15,20-tetrakis(pentafluorophenyl)porphyrinate (Scheme 1).

Scheme 1. Syntheses of 1−4 at −60 °C

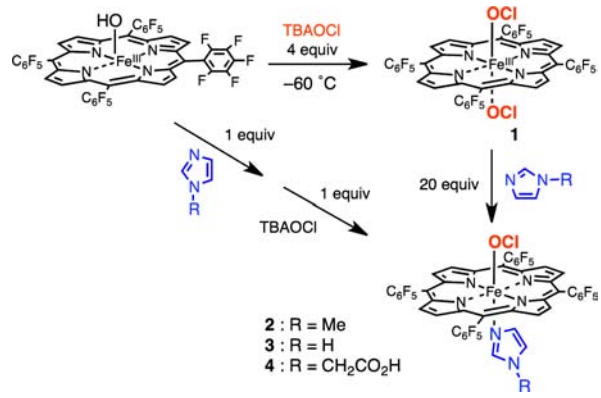

Figure 1 shows absorption spectral changes for the reaction of $(TPFP)Fe^{III}OH$ with tetrabutylammonium hypochlorite (TBAOCl) in 1:1 CH_2Cl_2/MeCN at −60 °C. $(TPFP)Fe^{III}OH$ shows a Soret band at 403 nm and a visible band at 564 nm, in accordance with the previous report.[11] Upon the addition of 4 equiv of TBAOCl, $(TPFP)Fe^{III}OH$ is quickly converted to a new compound, **1**, which exhibits a Soret band at 422 nm and a visible band at 534 nm. The absorption spectrum of **1** is close to that of the iodosylbenzene (O−I−Ph) adduct of iron(III) porphyrin complex.[12] **1** could also be prepared from $(TPFP)Fe^{III}OH$ and NaOCl/MeCN solution [Figure S1 in the Supporting Information (SI)]. **1** was found to be stable for 1 h at −60 °C but slowly decomposed to give an oxoiron(IV) porphyrin species, $(TPFP)Fe^{IV}$=O, exhibiting a Soret band at 414 nm and a visible band at 546 nm with clear isosbestic points at −40 °C

Received: November 5, 2012
Published: December 7, 2012

dx.doi.org/10.1021/ja3108774 | J. Am. Chem. Soc. 2012, 134, 20617−20620

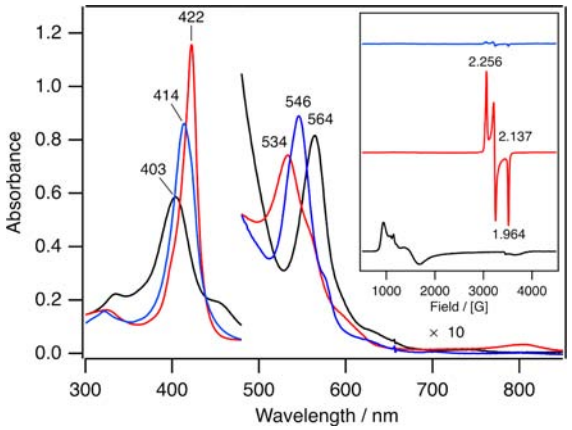

Figure 1. Absorption spectral changes for the formation and decomposition of **1** at −60 °C. Black line, (TPFP)Fe^{III}OH (5.0×10^{-5} M in a 0.1 cm UV cell); red and blue lines, **1** before and after thermal decomposition, respectively. Inset: EPR spectra of the corresponding complexes (5.0×10^{-4} M) at 4 K.

(Figures 1 and S2).[9,11,13] The time course of the absorbance for the decomposition reaction was fitted to a single-exponential function (Figure S2). These results suggested that **1** is a hypochloritoiron(III) porphyrin complex.

Insights into the structure of **1** were gained from further spectroscopic studies. Figure 2 shows ^{2}H and ^{19}F NMR spectra

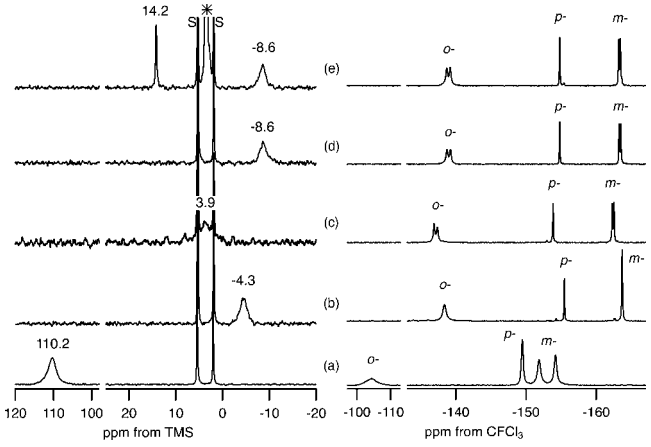

Figure 2. (left) ^{2}H and (right) ^{19}F NMR spectra of **1** and **2** ^{2}H-labeled at the pyrrole β positions in 1:1 CH_2Cl_2/MeCN at −60 °C: (a) (py-d_8-TPFP)Fe^{III}(OH) (5.0×10^{-4} M); (b) **1** prepared from (py-d_8-TPFP)Fe^{III}(OH) and TBAOCl (4 equiv); (c) (py-d_8-TPFP)Fe^{IV}=O formed from thermal decomposition; (d) **2** prepared from **1** and 1-MeIm (20 equiv); (e) **2** prepared from **1** and 1-d_3-MeIm (20 equiv). S = solvent peak; * = free 1-d_3-MeIm.

for the reaction of (py-d_8-TPFP)Fe^{III}OH with TBAOCl at −60 °C, where py-d_8-TPFP denotes TPFP labeled with ^{2}H at the eight pyrrole β positions. (py-d_8-TPFP)Fe^{III}OH showed a large downfield shift of the pyrrole β-^{2}H signal at 110.2 ppm (from tetramethylsilane), which is typical for a high-spin Fe^{III} porphyrin complex. Upon the addition of 4 equiv of TBAOCl, this signal disappeared, and a new signal appeared at −4.3 ppm. The disappearance of this signal upon thermal decomposition at −40 °C was accompanied by the appearance of a new ^{2}H NMR signal at 3.9 ppm, which is consistent with the pyrrole β-^{2}H signal for (py-d_8-TPFP)Fe^{IV}=O.[9a,11] These results clearly indicate that the pyrrole β-^{2}H NMR signal at −4.3 ppm corresponds to **1**. ^{19}F NMR spectra of the same samples afforded more structural information for **1** (Figure 2). (py-d_8-TPFP)Fe^{III}OH showed two ^{19}F NMR signals for the meta position of the *meso*-pentafluorophenyl groups, which is reasonable for five-coordinate (TPFP)Fe^{III}OH. The ^{19}F NMR signals corresponding to the ortho and meta positions of **1** were both observed as single peaks, indicating a symmetric axial coordination environment. This suggests that **1** is the bis(hypochlorito)iron complex [(TPFP)Fe^{III}(OCl)$_2$]$^-$. The ^{19}F NMR spectrum of (TPFP)-Fe^{IV}=O formed by thermal decomposition of **1** indicated an asymmetric axial ligand environment. The absence of other signals except for solvent peaks in the ^{2}H and ^{19}F NMR spectra of **1** indicated the absence of other side products.

The oxidation and spin states of **1** were studied by electron paramagnetic resonance (EPR) spectroscopy. **1**, prepared from (TPFP)Fe^{III}OH and 4 equiv of TBAOCl in 1:1 CH_2Cl_2/MeCN, has an EPR spectrum with a small g anisotropy (g = 2.256, 2.137, and 1.964) at 4 K, indicating low-spin Fe^{III} (Figure 1 inset). These EPR signals disappeared upon thermal decomposition to give (TPFP)Fe^{IV}=O, confirming the assignment as **1**. The EPR spectrum of **1** is similar to those of end-on low-spin peroxoiron(III) porphyrin complexes.[14] This is quite reasonable because OCl$^-$ and O_2^{2-} have similar electron configurations with occupied π^* orbitals. The low-spin Fe^{III} state of **1** is consistent with its ^{2}H and ^{19}F NMR shifts. The same EPR spectrum was obtained when **1** was prepared from (TPFP)Fe^{III}OH and NaOCl/MeCN solution (Figure S3).

1 was further characterized by resonance Raman (rR) spectroscopy. Figure 3 shows the rR spectra of **1** prepared

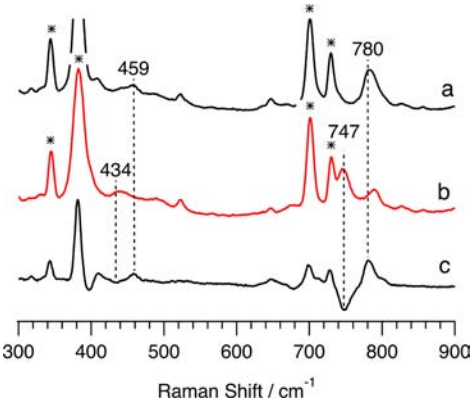

Figure 3. Resonance Raman spectra of (a) **1** and (b) ^{18}O-labeled **1** in 1:1 CH_2Cl_2/MeCN at −60 °C and (c) the difference spectrum (a − b). Peaks labeled with * originated from the solvent. λ_{ex} = 441.6 nm. Each spectrum shown is the sum of five spectra for five independent samples, each obtained with an exposure time of 60 s. For details, see the SI.

from TBA^{16}OCl and TBA^{18}OCl and their difference at −60 °C. The difference spectrum clearly reveals two sets of isotope-sensitive bands. One of these appeared at 780 cm^{-1} with ^{16}OCl$^-$ and shifted to 747 cm^{-1} with ^{18}OCl$^-$. The observed shift ($\Delta\nu$ = 33 cm^{-1}) is in good agreement with the calculated value of 30 cm^{-1} expected for a diatomic O−Cl oscillator.[15] Upon thermal decomposition to (TPFP)Fe^{IV}=O, the 780 cm^{-1} band of ^{16}OCl$^-$ disappeared, and a new band appeared at 828 cm^{-1}, which shifted to 791 cm^{-1} for the decomposition of ^{18}O-labeled **1** (Figure S4). The 828 cm^{-1} band could be easily assigned as the ν(Fe=O) band of (TPFP)Fe^{IV}=O. Moreover, in the accumulation of rR spectra, the band at 780 cm^{-1} gradually disappeared and the ν(Fe=O) band at 828 cm^{-1} gradually

dx.doi.org/10.1021/ja3108774 | J. Am. Chem. Soc. 2012, 134, 20617−20620

appeared (Figure S5). This is probably due to photodecomposition of **1** by the laser irradiation. These observations clearly indicate that the band at 780 cm^{-1} results from **1** and is assignable to the O−Cl stretching mode of the heme-bound OCl^-. The other isotope-sensitive band appeared at 459 cm^{-1} with $^{16}OCl^-$ and shifted to 434 cm^{-1} with $^{18}OCl^-$. The observed shift ($\Delta\nu$ = 25 cm^{-1}) is in good agreement with the calculated value of 26 cm^{-1} expected for a triatomic O−Fe−O oscillator.[15] This band, which also disappeared upon thermal or photodecomposition (Figure S6), can be assigned as the O−Fe−O symmetric stretch of the heme-bound hypochlorites in **1**.

We also performed electrospray ionization mass spectrometry (ESI-MS) analysis of **1**, but no negative ion peak corresponding to $[(TPFP)Fe^{III}(OCl)_2]^-$ was observed (Figure S7).

All of these spectroscopic data for **1** strongly support the formation of a bis(hypochlorito)iron(III) porphyrin complex, $[(TPFP)Fe^{III}(OCl)_2]^-$, by the reaction of $(TPFP)Fe^{III}OH$ with TBAOCl or NaOCl/MeCN solution.

To make a model complex for the hypochloritoiron(III) porphyrin intermediate of MPO, we prepared hypochloritoiron(III) porphyrin complexes with Im derivatives as axial ligands (**2**−**4** in Scheme 1). When 20 equiv of 1-methylimidazole (1-MeIm) was added to **1**, which had been prepared from $(TPFP)Fe^{III}OH$ and 4 equiv of TBAOCl in 1:1 CH_2Cl_2/MeCN at −60 °C, the absorption spectrum of **1** slowly changed to a new spectrum corresponding to **2** over the course of 2 h with clear isosbestic points (Figures 4 and S8). The absorption

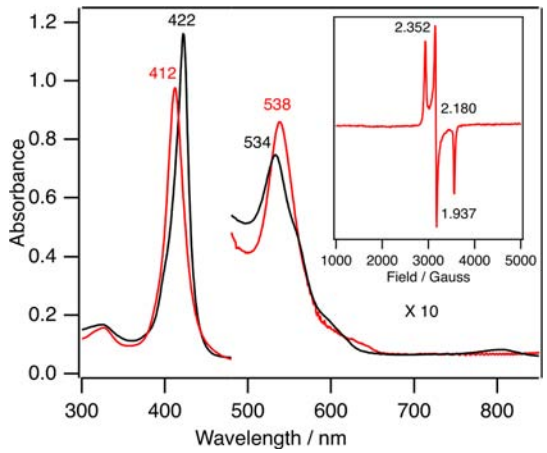

Figure 4. Absorption spectra of **1** (5.0×10^{-5} M in a 0.1 cm UV cell; black) and **2** prepared from **1** and 20 equiv of 1-MeIm (red) at −60 °C. Inset: EPR spectrum of **2** (5.0×10^{-4} M) in 1:1 CH_2Cl_2/MeCN at 4 K.

spectrum of **2** shows a Soret band at 412 nm and a visible band at 538 nm. Alternatively, **2** could be prepared from $(TPFP)Fe^{III}OH$ by sequential addition of 1 equiv of 1-MeIm and TBAOCl (Figure S9). Although **1** decomposed to $(TPFP)Fe^{IV}$═O within 1 h at −40 °C, **2** was found to be stable for hours even at −20 °C. **2** was further investigated by ^2H and ^{19}F NMR, EPR, and rR spectroscopy and ESI-MS. The pyrrole β-^2H signal of **2** was observed at −8.6 ppm at −60 °C (Figure 2d). This signal is different from those of **1**, $(TPFP)Fe^{III}(1\text{-MeIm})_2$, and $(TPFP)(1\text{-MeIm})Fe^{IV}$═O.[16] When 1-MeIm with a ^2H-labeled Me group (1-d_3-MeIm) was used for the preparation of **2**, a new paramagnetically shifted ^2H signal was observed at 14.2 ppm (Figure 2e), providing direct evidence for the coordination of 1-MeIm in **2**. The ^2H NMR shift of **2** was also different from the shifts of free 1-d_3-MeIm, $(TPFP)Fe^{III}(1\text{-MeIm})_2$, and $(TPFP)(1\text{-MeIm})Fe^{IV}$═O.[16] The ^{19}F NMR signals corresponding to the ortho and meta positions of **2** were observed as two peaks. This clearly indicates an asymmetric axial ligand environment (Figure 2d), consistent with OCl^- and 1-MeIm mixed ligand coordination in **2**. The absence of other NMR signals in the NMR spectra showed that decomposition did not occur upon the addition of 1-MeIm. **2** exhibited EPR signals at g = 2.352, 2.180, and 1.937 (Figure 4), with a g anisotropy slightly larger than that of **1** but still smaller than those of typical low-spin Fe^{III} complexes.[17] The absorption, ^2H NMR, and EPR spectra of **3** and **4**, which were similarly prepared by addition of imidazole and 1-imidazole acetic acid to **1** at −60 °C, were very close to those of **2** (Figures S10 and S11). No ESI-MS peak corresponding to **2** or **3** was detected because of its neutral character. However, **4** exhibited a negative ESI-MS peak at m/z 1204.12 (Figure S12). The peak location and isotope pattern were consistent with the ion $[C_{49}H_{13}N_6F_{20}FeO_3Cl]^-$, which is identical to the negative ion that would be formed by deprotonation of the 1-carboxymethyl group of **4**. The ion peak shifted by 2 mass units to m/z 1206.13 when $TBA^{18}OCl$ was used to prepare **4**, providing direct evidence that one OCl^- was bound to the heme iron even after addition of the imidazole. Finally, the rR spectra of **2** were obtained using various excitation wavelengths (442, 532, and 590 nm) at −60 °C and found to be almost identical to that of $(TPFP)(1\text{-MeIm})Fe^{IV}$═O, probably because laser irradiation during the rR measurements caused rapid decomposition of **2** to give $(TPFP)(1\text{-MeIm})Fe^{IV}$═O (Figures S13−S16). The spectroscopic data for **2**−**4** are fully consistent with the formation of iron(III) porphyrin complexes with OCl^- and an Im derivative as the axial ligands.

To investigate the reactivities of **1** and **2**, we examined their reactions with various organic substrates at low temperature (Scheme 2). **1** was found to react quickly with thioanisole at −60 °C. Upon the addition of 20 equiv of thioanisole, the absorption and ^2H NMR spectra of **1** changed within 1 min to spectra typical of a mixture of ferric porphyrin complexes, which were assigned as $(TPFP)Fe^{III}Cl$ and $(TPFP)Fe^{III}OH$ on the basis of their ^2H NMR shifts (Figure S17). Product analysis of the reaction mixture indicated the formation of methyl phenyl sulfoxide (MPS) in 78% yield. Although a significant yield (41%) of MPS was also obtained with only TBAOCl at −60 °C, this result reveals that **1** can oxidize sulfide to sulfoxide. The reaction with the ^{18}O-labeled **1** produced ^{18}O-labeled MPS (Figure S18), clearly indicating the transfer of the O atom of heme-bound OCl^- in the reaction. **1** was found to react with 1,3,5-

Scheme 2. Reactions of 1 and 2 with Various Organic Substrates[a]

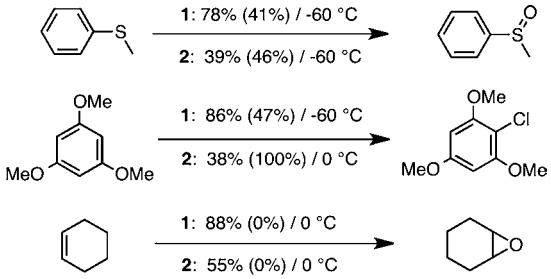

[a]Yields are based on TBAOCl used for synthesis of **1** (4 equiv) and **2** (1 equiv). The numbers in parentheses are yields of blank experiments. For details, see the SI.

dx.doi.org/10.1021/ja3108774 | J. Am. Chem. Soc. 2012, 134, 20617−20620

trimethoxybenzene at −60 °C, although this reaction was found to be much slower than that with thioanisole and required 2 h for completion. The absorption and ^{2}H NMR spectra of the final reaction solution showed the formation of a mixture of (TPFP)Fe^{III}Cl and (TPFP)Fe^{III}OH (Figure S19), and product analysis showed the formation of 1-chloro-2,4,6-trimethoxybenzene in 86% yield. Although the same compound was produced in 47% yield with only TBAOCl at −60 °C, the result indicates that **1** can chlorinate aromatic compounds. **1** was also mixed with cyclohexene, but the reaction did not proceed at −60 °C. When the reaction mixture was warmed to −20 °C, the reaction proceeded to completion, affording a mixture of (TPFP)Fe^{III}Cl and (TPFP)Fe^{III}OH (Figure S20). Product analysis showed the formation of cyclohexene oxide, 2-cyclohexen-1-ol, and 2-cyclohexen-1-one in yields of 63, 10, and 7%, respectively. 3-Chlorocyclohexene was not produced in the reaction. At 0 °C, the yield of cyclohexene oxide increased to 88%, but the yields of other products were unchanged. The reaction with only TBAOCl under the same conditions did not form cyclohexene oxide but instead gave 2-cyclohexen-1-ol and 2-cyclohexen-1-one in similar yields. The reaction with ^{18}O-labeled **1** resulted in ^{18}O incorporation only in cyclohexene oxide (Figure S21). In addition, while **1** reacted with cyclohexene within 3 min at −20 °C, (TPFP)Fe^{IV}=O formed from the decomposition of **1** required more than 90 min under the same conditions (Figure S22). These results indicate that **1** oxidizes cyclohexene to cyclohexene oxide and that the other products are due to side reactions such as radical chain reactions with contaminated oxygen gas. In fact, yields of >100% for 2-cyclohexen-1-ol and 2-cyclohexen-1-one were obtained when the reaction was carried out under air. Thus, **1** oxidizes olefins to epoxides.

We also examined the same reactions for **2** (Scheme 2). The reactivity of **2** with organic substrates was much lower than that of **1**. **2** reacted with thioanisole at −60 °C, but the reaction required ∼1 h to reach completion (Figures S23 and S24) and the yield (41%) was close to that of a blank experiment. **2** did not react with 1,3,5-trimethoxybenzene or cyclohexene at −60 °C. At 0 °C, **2** decomposed with concomitant formation of 1-chloro-2,4,6-trimethoxybenzene in 38% yield, but this was much lower than the quantitative yield (∼100%) of the blank experiment (Figure S25). On the other hand, cyclohexene was oxidized to cyclohexene oxide (55%), 2-cyclohexen-1-ol (64%), and 2-cyclohexen-1-one (197%) (Figure S26). The blank and ^{18}O-labeling experiments showed that **2** oxidized cyclohexene to cyclohexene oxide and that the other products were due to side reactions such as radical chain reactions with contaminated oxygen gas (Figure S27).

In summary, we obtained new hypochloritoiron(III) porphyrin complexes by reacting (TPFP)Fe^{III}OH with TBAOCl, and the structures of these complexes were characterized by various spectroscopic methods. The reactivity study revealed that the OCl^- complexes are capable of sulfoxidation, chlorination, and epoxidation reactions and that the nature of the other axial ligand influences the reactivity.

■ ASSOCIATED CONTENT

Supporting Information

Figure S1−S27 and experimental details. This material is available free of charge via the Internet at http://pubs.acs.org.

■ AUTHOR INFORMATION

Corresponding Author

hiro@ims.ac.jp

Notes

The authors declare no competing financial interest.

■ ACKNOWLEDGMENTS

This study was supported by JSPS (Grant-in-Aid for Scientific Research, Grant 22350030).

■ REFERENCES

(1) (a) Dunford, H. B. *Heme Peroxidases*; Wiley-VCH: New York, 1999. (b) Dawson, J. H.; Sono, M. *Chem. Rev.* **1987**, *87*, 1255.

(2) (a) Klebanoff, S. J. *J. Leukocyte Biol.* **2005**, *77*, 598. (b) Hampton, M. B.; Kettle, A. J.; Winterbourn, C. C. *Blood* **1998**, *92*, 3007. (c) Malle, E.; Furtmüller, P. G.; Sattler, W.; Obinger, C. *Br. J. Pharmacol.* **2007**, *152*, 838.

(3) Hofrichter, M.; Ullrich, R. *Appl. Microbiol. Biotechnol.* **2006**, *71*, 276.

(4) (a) Marquez, L. A.; Huang, J. T.; Dunford, H. B. *Biochemistry* **1994**, *33*, 1447. (b) Palcic, M. M.; Rutter, R.; Araiso, T.; Hager, L. P.; Dunford, H. B. *Biochem. Biophys. Res. Commun.* **1980**, *94*, 1123. (c) Rutter, R.; Hager, L. P. *J. Biol. Chem.* **1982**, *257*, 7958.

(5) (a) Furtmüller, P. G.; Obinger, C.; Hsuanyu, Y.; Dunford, H. B. *Eur. J. Biochem.* **2000**, *267*, 5858. (b) Marquez, L. A.; Dunford, H. B. *J. Biol. Chem.* **1995**, *270*, 30434. (c) Furtmüller, P. G.; Burner, U.; Obinger, C. *Biochemistry* **1998**, *37*, 17923. (d) Lambeir, A.-M.; Dunford, H. B. *J. Biol. Chem.* **1983**, *258*, 13558. (e) Dunford, H. B.; Lambeir, A.-M.; Kashem, M. A.; Pickard, M. *Arch. Biochem. Biophys.* **1987**, *252*, 292.

(6) (a) Meunier, B. *Chem. Rev.* **1992**, *92*, 1411. (b) Meunier, B.; Guilmet, E.; Carvalho, M.-E. D.; Poilblanc, R. *J. Am. Chem. Soc.* **1984**, *106*, 6668. (c) Adam, W.; Roschmann, K. J.; Saha-Moller, C. R.; Seebach, D. *J. Am. Chem. Soc.* **2002**, *124*, 5068. (d) Jacobsen, E. N.; Zhang, W.; Muci, A. R.; Ecker, J. R.; Deng, L. *J. Am. Chem. Soc.* **1991**, *113*, 7063.

(7) Jin, N.; Bourassa, J. L.; Tizio, S. C.; Groves, J. T. *Angew. Chem., Int. Ed.* **2000**, *39*, 3849.

(8) (a) Wagenknecht, H. A.; Woggon, W. D. *Chem. Biol.* **1997**, *4*, 367. (b) Wagenknecht, H. A.; Woggon, W. D. *Angew. Chem., Int. Ed. Engl.* **1997**, *36*, 390.

(9) (a) Cong, Z.; Kurahashi, T.; Fujii, H. *Angew. Chem., Int. Ed.* **2011**, *50*, 9935. (b) Cong, Z.; Kurahashi, T.; Fujii, H. *J. Am. Chem. Soc.* **2012**, *134*, 4469.

(10) (a) Volz, H.; Müller, W. *Chem. Ber.* **1997**, *130*, 1099. (b) Liu, W.; Groves, J. T. *J. Am. Chem. Soc.* **2010**, *132*, 12847. (c) Cho, J.; Jeon, S.; Wilson, S. A.; Liu, L. V.; Kang, E. A.; Braymer, J. J.; Lim, M. H.; Hedman, B.; Hodgson, K. O.; Valentine, J. S.; Solomon, E. I.; Nam, W. *Nature* **2011**, *478*, 502. (d) Wang, C.; Kurahashi, T.; Fujii, H. *Angew. Chem., Int. Ed.* **2012**, *51*, 7809.

(11) Pan, Z.; Newcomb, M. *Inorg. Chem.* **2007**, *46*, 6767.

(12) Nam, W.; Choi, S. K.; Lim, M. H.; Rohde, J. U.; Kim, I.; Kim, J.; Kim, C.; Que, L., Jr. *Angew. Chem., Int. Ed.* **2003**, *42*, 109.

(13) (a) Nam, W.; Park, S.-E.; Lim, I. K.; Lim, M. H.; Hong, J.; Kim, J. *J. Am. Chem. Soc.* **2003**, *125*, 14674. (b) Nam, W.; Lim, M. H.; Oh, S.-Y.; Lee, J. H.; Lee, H. J.; Woo, S. K.; Kim, C.; Shin, W. *Angew. Chem., Int. Ed.* **2000**, *39*, 3646.

(14) (a) Davydov, R.; Satterlee, J.; Fujii, H.; Sauer-Masarwa, A.; Busch, D. H.; Hoffman, B. M. *J. Am. Chem. Soc.* **2003**, *125*, 16340. (b) Liu, J.-G.; Shimizu, Y.; Ohta, T.; Naruta, Y. *J. Am. Chem. Soc* **2010**, *132*, 3672. (c) Liu, J.-G.; Ohta, T.; Yamaguchi, S.; Ogura, T.; Sakamoto, S.; Naruta, Y. *Angew. Chem., Int. Ed.* **2009**, *48*, 9262.

(15) Spiro, T. G.; Czernuszewicz, R. S. In *Physical Methods in Bioinorganic Chemistry*; Que, L., Jr., Ed.; University Science Books: Mill Valley, CA, 2000.

(16) (a) La Mar, G. N.; Satterlee, J. D. *J. Am. Chem. Soc.* **1976**, *98*, 2804. (b) Balch, A. L.; La Mar, G. N.; Latos-Grazynski, L.; Renner, M. W.; Thanabal, V. *J. Am. Chem. Soc.* **1985**, *107*, 3003.

(17) Palmer, G. P. In *Iron Porphyrins, Part II*; Lever, A. B. P., Gray, H. B., Eds.; Addison-Wesley: London, 1983.